

Power emitted by a multipole near an interface

Henk F. Arnoldus *

Department of Physics and Astronomy, Mississippi State University, P.O. Drawer 5167, Mississippi State, MS 39762-5167, USA

Received 14 July 2004; accepted for publication 20 August 2004

Available online 11 September 2004

Abstract

The power emitted by an electric or a magnetic multipole of arbitrary order located near an interface with a layer on a substrate is studied. The power in the far field can be expressed in terms of Fresnel reflection and transmission coefficients for plane waves. When eliminating the transmission coefficients in favor of the reflection coefficients and combining the various contributions, it appears that the power has three distinct parts: (i) the first term is the power emitted by an unbounded multipole, and the process of reflection and transmission redistributes the angular dependence of this power; (ii) the second term represents the interference between the multipole waves which travel directly towards a detector and the waves which are reflected by the interface, a mechanism which modifies the emission rate, primarily depending on the distance between the multipole and the interface; (iii) the third term accounts for evanescent multipole waves which are converted into traveling waves upon transmission through the layer. When the distance between the multipole and the interface is about or less than a fraction of a wavelength, this third term can be extremely large compared to the emission rate by an unbounded multipole (for which all power comes from traveling multipole waves).

© 2004 Elsevier B.V. All rights reserved.

Keywords: Atom–solid interactions; Dielectric phenomena; Light scattering; Photon emission; Metallic surfaces; Metal–insulator interfaces

1. Introduction

An atom with an oscillating electric dipole moment emits electric dipole radiation. The radiative power emitted by the atom does not only depend on the dipole moment, but also on the surroundings of the atom, an observation first made by Pur-

cell [1] in a quantum–mechanical context. When the atom is located near the boundary of a dielectric or metallic medium, then part of the radiation will reflect at the interface, leading to constructive or destructive interference with the radiation emitted directly by the atom towards a detector in the far field. The interference depends on the distance between the atom and the surface of the interface. In addition, when the interface consists of a layer of material on a transparent substrate, part of

* Tel.: +1 662 325 2919; fax: +1 662 325 8898.

E-mail address: arnoldus@ra.msstate.edu

the radiation will be transmitted through the layer and into the substrate. The modifications of the angular distribution of the power and the total emitted power by an electric dipole due to the presence of an interface have been studied extensively by a variety of methods [2–7] and in particular the dependence on the atom–surface separation distance has attracted a great deal of attention. The theoretical predictions have been verified experimentally for both radio-wave and optical frequencies [8–15]. In this paper we generalize these results by considering the power emitted by an electric or a magnetic multipole of arbitrary order, located near an interface.

The problem of reflection and transmission of multipole radiation by an interface is most conveniently approached by means of an angular spectrum representation of the multipole field. This is an integral representation (superposition) in which each partial wave is a plane wave [16]. The independent variable is k_{\parallel} , which is the parallel part with respect to the surface, taken to be the xy -plane, of the wave vector k of the incident wave, and the integration runs over the entire k_{\parallel} -plane. When the multipole is embedded in a medium with dielectric constant ϵ_1 , assumed to be positive and corresponding to an index of refraction $n_1 = \sqrt{\epsilon_1}$, then the wave number is $k = n_1 k_0$, where $k_0 = \omega/c$ and ω is the angular frequency of the oscillations of the dipole moment. The z -component of the wave vector k is then $k_z = \pm(k^2 - k_{\parallel}^2)^{1/2}$. For $k_{\parallel} < k$, the value of k_z is real and we have a traveling wave. We select the positive or negative sign such that the wave travels away from the multipole in both the positive and negative z -directions. On the other hand, for $k_{\parallel} > k$, the variable k_z becomes imaginary, and the sign is chosen in such a way that the wave decays exponentially away from the multipole in both the positive and negative z -directions. These are the evanescent waves of the angular spectrum representation.

We shall consider the situation depicted in Fig. 1, where the multipole is located a distance H above the interface, and is embedded in a medium with index of refraction n_1 . The region $-L < z < 0$ is a layer with dielectric constant ϵ_2 , and the substrate has a dielectric constant ϵ_3 . We assume that all dielectric constants are real, thereby excluding

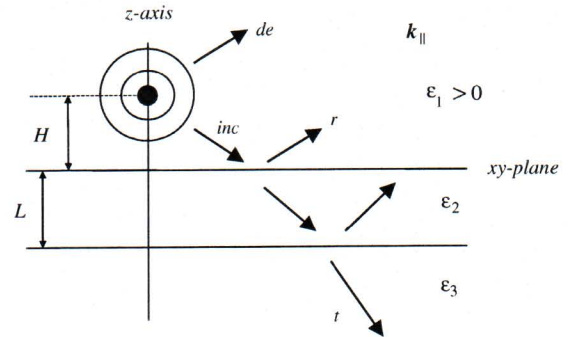


Fig. 1. The multipole is located on the z -axis, a distance H above the xy -plane, and the circles indicate the multipole radiation which consists of spherical waves. The multipole is embedded in a medium with dielectric constant ϵ_1 , the layer occupies the region $-L < z < 0$ and has a dielectric constant ϵ_2 , and the substrate has dielectric constant ϵ_3 . In an angular spectrum representation, the radiation in each region is a superposition of plane waves, and this is schematically indicated by the arrows. When a partial wave is traveling, the arrow indicates the wave vector, but when the wave is evanescent, the wave travels parallel to the xy -plane with wave vector k_{\parallel} , and decays in the $+z$ - or $-z$ -direction. For a given incident wave, each wave vector has the same parallel part k_{\parallel} as the incident wave. The de -waves are emitted by the multipole towards a detector in the far field, and the inc -waves are the incident waves which reflect at the interface, giving rise to the specular r -waves. Each incident wave gives a transmitted t -wave, which, when traveling, contributes to the power in $z < -L$.

possible absorption, but we allow for the possibility that either ϵ_2 or ϵ_3 , or both, are negative. In particular, a negative ϵ_3 models a metallic substrate. The reflected and transmitted waves and the waves in the layer are also plane waves, given an incident plane wave, and the boundary conditions at $z = 0$ and $z = -L$ require that all waves have wave vectors with the same k_{\parallel} as the incident wave. We shall use the notation $\alpha = k_{\parallel}/k_0$ for the dimensionless magnitude of k_{\parallel} .

In a medium with dielectric constant ϵ_j , the dispersion relation is $k_j^2 = \epsilon_j k_0^2$ and, given k_{\parallel} , this determines the z -component of the corresponding wave vector k_j , apart from its sign, since $k_j^2 = k_{\parallel}^2 + k_{z,j}^2$. When ϵ_j is negative, the z -component is imaginary for all k_{\parallel} , and there can only exist evanescent waves in the medium. For positive ϵ_j , the wave is traveling ($k_{z,j}$ real) for $k_{\parallel} < n_j k_0$, with $n_j = \sqrt{\epsilon_j}$, and evanescent ($k_{z,j}$ imaginary) for $k_{\parallel} > n_j k_0$. In terms of α , this is $\alpha < n_j$ and $\alpha > n_j$,

respectively. A useful dimensionless variable for the waves in the material with dielectric constant ε_j is

$$v_j = \sqrt{\varepsilon_j - \alpha^2}, \quad (1)$$

with the understanding that the square root is taken as positive imaginary if its argument is negative. The value of the z -component of a wave vector in medium ε_j is then $k_{zj} = \pm k_0 v_j$, given α , and the sign of k_{zj} depends on whether the wave travels/decays in the positive or negative z -direction. When v_j is positive, the corresponding wave is traveling, and when v_j is positive imaginary the wave is evanescent.

When ε_3 is negative, the parameter v_3 is imaginary for all α . Then the waves in the substrate are evanescent, and do not contribute to the emitted power. Let us now consider $\varepsilon_3 > 0$. When the incident wave in medium ε_1 is traveling we have $0 \leq \alpha < n_1$, and the angle of incidence θ_i is given by $\alpha = n_1 \sin \theta_i$. The waves in the substrate can be traveling or evanescent, depending on the value of k_{\parallel} of the incident wave, or α . If the transmitted wave is traveling, then the angle of transmission θ_t is given by $\alpha = n_3 \sin \theta_t$, since both the incident and transmitted wave must have the same k_{\parallel} . Therefore we have $\alpha = n_3 \sin \theta_t = n_1 \sin \theta_i$ which is Snell's law. For $n_3 < n_1$ there exists an angle of incidence for which the angle of transmission becomes $\pi/2$. This is the critical angle θ_c , given by

$$\sin \theta_c = \frac{n_3}{n_1}. \quad (2)$$

If the angle of incidence of a traveling plane wave exceeds θ_c , then the transmitted wave in the substrate becomes evanescent. These waves die out exponentially in the negative z -direction, and do not contribute to the radiated power in the far field. Similarly, for $n_3 > n_1$, there exists an angle of transmission for which the angle of incidence becomes $\pi/2$. We define an angle θ_{ac} by

$$\sin \theta_{ac} = \frac{n_1}{n_3}. \quad (3)$$

This angle θ_{ac} has the significance that if a traveling wave in medium n_3 is detected at a transmission angle larger than θ_{ac} , it must have its origin in an evanescent incident wave in medium n_1 . Since

this is just the opposite effect as compared to the situation with the critical angle, we have called this angle θ_{ac} the anti-critical angle [17]. Therefore, such evanescent waves of the multipole field contribute to the emitted power, since they are converted by the interface into traveling waves which end up in the far field in the substrate. With $\alpha = n_3 \sin \theta_t$ and $0 \leq \theta_t < \pi/2$ we see that the range of α values in the angular spectrum contributing to the transmitted traveling waves is $0 \leq \alpha < n_3$. On the other hand, the incident waves are traveling for $0 \leq \alpha < n_1$, and therefore α values in the range $n_1 < \alpha < n_3$ represent the combination of evanescent incident waves and traveling transmitted waves.

The power emitted by a multipole comes from traveling waves in the angular spectrum which travel directly towards the detector (the *de*-waves in Fig. 1), and traveling waves which reflect first at the interface and then travel towards the detector (the *r*-waves). Part of the incident traveling waves refract at the interface and contribute to the power transmitted by the layer. For the situation of $n_3 > n_1$, the power has the additional contribution from the emitted evanescent waves which are transformed into traveling waves by the interface. The contribution of the evanescent waves was considered in detail recently [18] for an electric dipole, and it was shown that under certain conditions the power due to evanescent waves can greatly exceed the power due to traveling waves.

2. Angular distribution of multipole radiation near an interface

The electromagnetic field of an electric or magnetic multipole in vacuum is well-known [19–22], and only slight modifications are needed to account for the embedding medium with index of refraction n_1 . For the problem of a multipole near an interface we need an angular spectrum representation of the multipole field, which can be obtained [23,24] with a theorem due to Erdélyi [25]. With an asymptotic expansion with the method of stationary phase [26,27] we then evaluate the field in the far zone, after which the emitted power per unit solid angle, $dP/d\Omega$, can be found by

evaluating the Poynting vector. The result can be written as

$$\frac{dP}{d\Omega} = P_1 \mathcal{N}_{\eta\ell m}(\hat{\mathbf{r}}), \quad (4)$$

where P_1 is the emitted power by the multipole in an unbounded medium with index of refraction n_1 and $\mathcal{N}_{\eta\ell m}(\hat{\mathbf{r}})$ is the normalized intensity as a function of the observation direction $\hat{\mathbf{r}}$. The value of P_1 is determined by the multipole moments of the source, and its explicit form is irrelevant for the present discussion. The possible values of ℓ are $1, 2, \dots$ for a dipole, quadrupole, \dots , and given ℓ the possible values of m are $m = -\ell, \dots, \ell$. We have added the subscript η to indicate magnetic ($\eta = 1$) and electric ($\eta = -1$) multipoles.

The explicit result for the intensity distribution of the radiation emitted in the half-space $z > H$ for the case of a magnetic multipole is [28]

$$\begin{aligned} \mathcal{N}_{1\ell m}(\hat{\mathbf{r}}) = & |1 + (-1)^{\ell+m} R_p(\alpha_1) e^{i\beta \cos \theta}|^2 f_{\ell m}(\cos \theta) \\ & + |1 - (-1)^{\ell+m} R_s(\alpha_1) e^{i\beta \cos \theta}|^2 g_{\ell m}(\cos \theta). \end{aligned} \quad (5)$$

This distribution depends on the polar angle θ with the positive z -axis, but is independent of the azimuthal angle ϕ . The distance H between the multipole and the surface enters only through the dimensionless parameter $\beta = 2n_1 k_0 H$. The Fresnel reflection coefficients R_σ , with $\sigma = s$ or p indicating the polarization of the corresponding plane wave, depend on the three dielectric constants, the dimensionless layer thickness $d = k_0 L$, and the parameter α . For a given observation angle θ , the Fresnel coefficients have to be evaluated at $\alpha_1 = n_1 \sin \theta$. This shows that the contribution from the reflected waves to the intensity at angle θ comes from a plane wave with angle of incidence $\theta_i = \theta$. Expression (5) clearly exhibits that the field is a superposition of de -waves, represented by the terms “1” inside the absolute value signs, and reflected waves. The factors $\exp(i\beta \cos \theta)$ account for the retardation of the r -waves with respect to the de -waves, and this leads to an interference pattern. Without the interface we have $R_\sigma = 0$, and Eq. (5) reduces to

$$\mathcal{N}_{1\ell m}(\hat{\mathbf{r}}) = f_{\ell m}(\cos \theta) + g_{\ell m}(\cos \theta), \quad (6)$$

which shows that the functions $f_{\ell m}$ and $g_{\ell m}$ account for the intensity distribution of a multipole in free space ($n_1 = 1$ and without boundaries). The explicit expressions for these functions, which in general have complex-valued arguments, are given in Ref. [24].

For $\varepsilon_3 < 0$ all radiation in the half-space $z < -L$ consists of evanescent waves, and no power is transmitted through the layer into the substrate. For $\varepsilon_3 > 0$, the intensity distribution in $z < -L$ can be expressed in terms of Fresnel transmission coefficients T_σ and the result for a magnetic multipole is

$$\begin{aligned} \mathcal{N}_{1\ell m}(\hat{\mathbf{r}}) = & \frac{n_3}{n_1} e^{\beta \text{Im } w} [|\hat{T}_p(\alpha_3)|^2 f_{\ell m}(w) \\ & + |\hat{T}_s(\alpha_3)|^2 g_{\ell m}(w)]. \end{aligned} \quad (7)$$

Here we have introduced the modified transmission coefficients

$$\hat{T}_\sigma(\alpha) = \frac{v_3}{v_1} T_\sigma(\alpha), \quad (8)$$

in terms of the parameters v_j from Eq. (1). The transmission coefficients have to be evaluated at $\alpha_3 = n_3 \sin \theta$, and since $\theta_t = \pi - \theta$ we have $\alpha_3 = n_3 \sin \theta_t$. The parameter w appearing as the arguments of the functions $f_{\ell m}$ and $g_{\ell m}$ is

$$w = -\sqrt{1 - (\varepsilon_3/\varepsilon_1) \sin^2 \theta}, \quad (9)$$

which is negative or negative imaginary. When the corresponding incident wave is traveling we have $n_1 \sin \theta_i = n_3 \sin \theta_t$, and this parameter is $w = -\cos \theta_i$. This shows that the amplitudes of the transmitted waves are determined by the amplitudes of the corresponding incident waves, as could be expected. We note that the functions $f_{\ell m}$ and $g_{\ell m}$ are even in their arguments, so that replacing w by $-w$ has no effect. On the other hand, for a transmission angle which corresponds to an evanescent incident wave (which can only happen for $\varepsilon_3 > \varepsilon_1$), the parameter w is imaginary. This is the case for $\theta_{ac} < \theta_t < \pi/2$. Then the overall factor $\exp(\beta \text{Im } w)$ decays exponentially with the distance H between the dipole and the surface, reflecting the fact that the evanescent waves from the multipole decay in the direction towards the surface. Without the interface we have

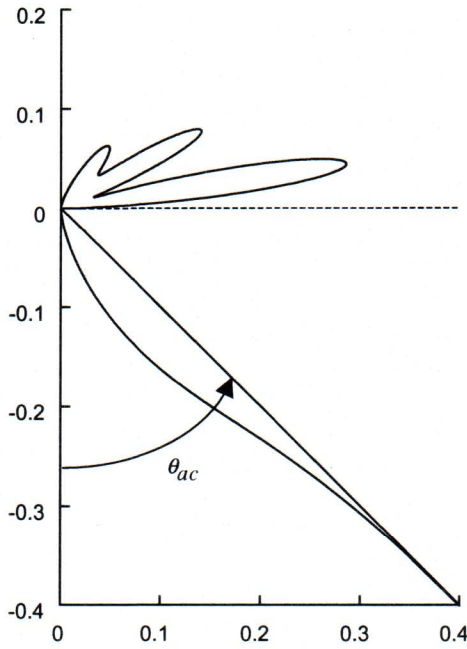


Fig. 2. The graph shows a polar diagram of the intensity distribution of an electric quadrupole with $m = 2$. The dielectric constants are $\varepsilon_1 = 1$, $\varepsilon_2 = \varepsilon_3 = 2$, for which the anti-critical angle is $\theta_{ac} = 45^\circ$. The parameter β is taken as 6π , corresponding to a normal distance of 1.5 wavelengths. Already for this relatively small value of the distance between the multipole and the interface, we see that almost no radiation is present in the region $\theta_{ac} < \theta < \pi/2$. The fraction f for these parameters is 0.73% (see Section 7, Eq. (30)).

$n_1 = n_2 = n_3$, and therefore $v_3 = v_1$, $\hat{T}_\sigma = T_\sigma = 1$, and $w = \cos \theta$ ($\cos \theta$ is negative for $z < -L$). Expression (7) then reduces to Eq. (6). For an electric multipole the same expressions hold, except that the Fresnel coefficients for s- and p-polarization in Eqs. (5) and (7) have to be exchanged. The intensity distribution is independent of the sign of m , so we shall consider $m \geq 0$ only. Fig. 2 shows a typical example of a radiation pattern for an electric quadrupole.

3. Emitted power

The power per unit solid angle is written as in Eq. (4) in terms of the normalized intensity distribution $\mathcal{N}_{\eta\ell m}(\hat{\mathbf{r}})$. Since the expressions for $\mathcal{N}_{\eta\ell m}(\hat{\mathbf{r}})$

are different for $z > H$ and $z < -L$ we split the emitted power accordingly. The emitted power in $z > H$ is

$$P_{\eta\ell m}^> = P_1 \int_0^{\pi/2} d\theta \int_0^{2\pi} d\phi \sin \theta \mathcal{N}_{\eta\ell m}(\hat{\mathbf{r}}), \quad (10)$$

in terms of the spherical coordinates (θ, ϕ) , and the power emitted in the direction $z < -L$ will be indicated by $P_{\eta\ell m}^<$ and is defined as in Eq. (10), with the integration limits for θ changed to $\pi/2 < \theta < \pi$. The total power is then given by $P_{\eta\ell m} = P_{\eta\ell m}^> + P_{\eta\ell m}^<$. The intensity distribution $\mathcal{N}_{\eta\ell m}(\hat{\mathbf{r}})$ is independent of ϕ , so the integration over ϕ gives 2π . We normalize the power with P_1 , and write the normalized power as $P_{\eta\ell m} = P_{\eta\ell m}/P_1$, and similarly for $P_{\eta\ell m}^>$ and $P_{\eta\ell m}^<$.

Without the interface the normalized intensity distribution is given by the right-hand side of Eq. (6) for all θ , and both for magnetic and electric multipoles. When integrated over a 4π solid angle this gives unity. Since the functions $f_{\ell m}$ and $g_{\ell m}$ are even in their arguments, it follows that the power emitted in the negative z -direction is equal to the power emitted in the positive z -direction, and therefore we have the identity

$$2\pi \int_0^{\pi/2} d\theta \sin \theta [f_{\ell m}(\cos \theta) + g_{\ell m}(\cos \theta)] = \frac{1}{2}. \quad (11)$$

For the emitted power in $z > H$ we use expression (5) for $\mathcal{N}_{1\ell m}(\hat{\mathbf{r}})$, and we change the integration variable θ to α according to $\alpha = n_1 \sin \theta$. We then have $n_1 \cos \theta = v_1$, and the terms that are independent of the Fresnel coefficients combine just as in Eq. (11). This yields for the normalized power in $z > H$ for a magnetic multipole

$$\begin{aligned} P_{1\ell m}^> = & \frac{1}{2} + \frac{2\pi}{n_1} \int_0^{n_1} d\alpha \frac{\alpha}{v_1} \langle |R_p(\alpha)|^2 \\ & + 2(-1)^{\ell+m} \text{Re}[R_p(\alpha)e^{i\beta v_1/n_1}] \rangle f_{\ell m}(v_1/n_1) \\ & + \{ |R_s(\alpha)|^2 - 2(-1)^{\ell+m} \text{Re}[R_s(\alpha)e^{i\beta v_1/n_1}] \} \\ & \times g_{\ell m}(v_1/n_1) \rangle. \end{aligned} \quad (12)$$

The term $1/2$ on the right-hand side accounts for the directly emitted waves by the multipole towards the far field in $z > H$, and the terms with $|R_\sigma(\alpha)|^2$ represent the power by the reflected waves.

The remaining terms with $R_\sigma(\alpha)\exp(i\beta v_1/n_1)$ are a result of interference between the *de*- and the *r*-waves.

For the power in $z < -L$, assuming that ε_3 is positive, we use expression (7) and set $\alpha = n_3 \sin \theta$. This gives $w = -v_1/n_1$, and we obtain for a magnetic multipole

$$P_{1\ell m}^< = \frac{2\pi}{n_1} \int_0^{n_3} d\alpha \frac{\alpha}{v_1} e^{-\beta \text{Im} v_1/n_1} \frac{v_3}{v_1^*} [|T_p(\alpha)|^2 f_{\ell m}(v_1/n_1) + |T_s(\alpha)|^2 g_{\ell m}(v_1/n_1)], \quad (13)$$

where we have used Eq. (8). For $z < -L$ there are only transmitted waves with an intensity proportional to $|T_\sigma(\alpha)|^2$. When a corresponding incident wave is traveling, v_1 is real, and $\exp(-\beta \text{Im} v_1/n_1) = 1$. On the other hand, when the incident wave is evanescent, this factor is real and decays exponentially with the distance β .

4. Fresnel reflection and transmission coefficients

The results from the previous section do not depend on the explicit forms of the Fresnel reflection and transmission coefficients. When considering the total emitted power, the various contributions can be combined in an appealing way by using properties of the Fresnel coefficients. Therefore we give here the reflection and transmission coefficients, and we express these in terms of the variables v_j , defined in Eq. (1). We have

$$R_s(\alpha) = \frac{1}{A_s} [(v_1 - v_2)(v_2 + v_3) + (v_1 + v_2)(v_2 - v_3)e^{2iv_2d}], \quad (14)$$

$$R_p(\alpha) = \frac{1}{A_p} [(\varepsilon_2 v_1 - \varepsilon_1 v_2)(\varepsilon_3 v_2 + \varepsilon_2 v_3) + (\varepsilon_2 v_1 + \varepsilon_1 v_2)(\varepsilon_3 v_2 - \varepsilon_2 v_3)e^{2iv_2d}], \quad (15)$$

$$T_s(\alpha) = \frac{4v_1 v_2}{A_s} e^{i(v_2 - v_3)d}, \quad (16)$$

$$T_p(\alpha) = \frac{4v_1 v_2}{A_p} \varepsilon_2 n_1 n_3 e^{i(v_2 - v_3)d}, \quad (17)$$

with

$$A_s = (v_1 + v_2)(v_2 + v_3) + (v_1 - v_2)(v_2 - v_3)e^{2iv_2d}, \quad (18)$$

$$A_p = (\varepsilon_2 v_1 + \varepsilon_1 v_2)(\varepsilon_3 v_2 + \varepsilon_2 v_3) + (\varepsilon_2 v_1 - \varepsilon_1 v_2)(\varepsilon_3 v_2 - \varepsilon_2 v_3)e^{2iv_2d}. \quad (19)$$

We have indicated in the notation the dependence on the variable α , since this will be the integration variable in the expression for the total power. The Fresnel coefficients depend furthermore parametrically on the dielectric constants ε_1 , ε_2 , ε_3 , and the dimensionless layer thickness d .

The variables v_j are the dimensionless perpendicular components of the various wave vectors, apart from a possible minus sign depending on the wave under consideration. When v_j is real, the corresponding wave is traveling and when v_j is imaginary the wave is evanescent in the z -direction. We therefore have $v_j^* = v_j$ for a traveling wave and $v_j^* = -v_j$ for an evanescent wave. From this observation a variety of relations for the Fresnel coefficients can be derived, and these are summarized in Fig. 3.

5. The three cases

The result for the total power can be simplified considerably with the help of the relations for the Fresnel coefficients from the previous section. We can add the power emitted in $z > H$ and $z < -L$, but the way in which these contributions combine depends on the character of the waves in the various regions. We have to distinguish three possible cases.

1. $\varepsilon_3 < 0$

When ε_3 is negative, as for instance for a metal (neglecting absorption), then all waves in $z < -L$ are evanescent, and no power is emitted in this region. We therefore have $P_{1\ell m} = P_{1\ell m}^>$, with $P_{1\ell m}^>$ given by Eq. (12). In this case, the incident and reflected waves are traveling and the transmitted waves are evanescent, which corresponds to the situation shown in Fig. 3a. We then notice that the terms with $|R_\sigma(\alpha)|^2 = 1$ in Eq. (12) give the integral of Eq. (11), and this yields the simplified expression for the power

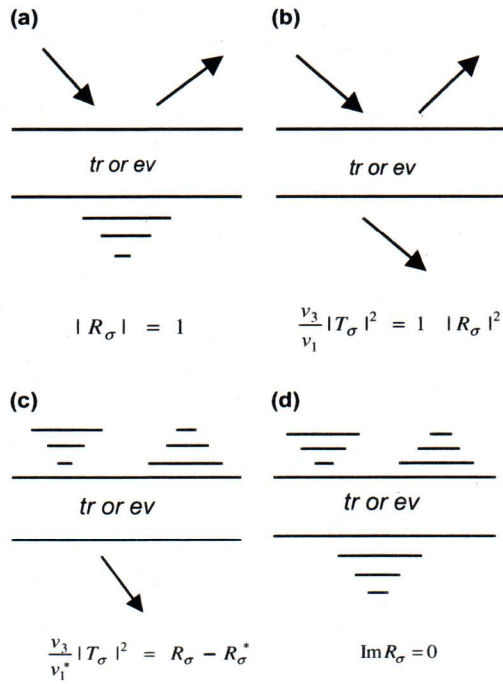


Fig. 3. The figure shows various relations for the Fresnel reflection and transmission coefficients. Whether a wave in the material with dielectric constant ε_j is traveling or evanescent depends on the value of the corresponding v_j , given by Eq. (1). When v_j is real, the wave is traveling, which is indicated by an arrow, and when v_j is imaginary, the wave is evanescent, which is indicated by dashes. It appears that the relations shown do not depend on whether the wave in the layer is traveling or evanescent, and the relations are the same for s- and p-polarization.

$$P_{1\ell m} = 1 + \frac{4\pi}{n_1} (-1)^{\ell+m} \text{Re} \int_0^{n_1} d\alpha \frac{\alpha}{v_1} e^{i\beta v_1/n_1} \times [R_p(\alpha) f_{\ell m}(v_1/n_1) - R_s(\alpha) g_{\ell m}(v_1/n_1)], \quad (20)$$

where we have used that the functions $f_{\ell m}$ and $g_{\ell m}$ are real.

2. $0 < \varepsilon_3 < \varepsilon_1$

For $\varepsilon_3 > 0$ there are traveling waves in $z < -L$ which contribute to the power. For $\varepsilon_3 < \varepsilon_1$ there exists a critical angle θ_c , given by Eq. (2), and for a given traveling incident wave, the corresponding transmitted wave can be traveling or evanescent. For the power in $z > H$ this affects the property of the Fresnel reflection coefficients. When $0 \leq \theta_i < \theta_c$, we have the situation of Fig. 3b, whereas for an evanescent transmitted wave, for

which $\theta_c < \theta_i < \pi/2$, we have again the case shown in Fig. 3a. The corresponding α ranges are $0 \leq \alpha < n_3$ and $n_3 < \alpha < n_1$, respectively. For the transmitted power the integration range is $0 < \alpha < n_3$, and this corresponds to the situation of Fig. 3b. We use the given equation to eliminate the transmission coefficients in favor of the reflection coefficients in Eq. (13) for the power in $z < -L$ (and use that v_1 is real here). For the terms with $|R_\sigma(\alpha)|^2$ in Eq. (12) we split the integral in an integral over $0 < \alpha < n_3$ and an integral over $n_3 < \alpha < n_1$. Then we find that the first integral cancels exactly against the terms in the expression for the power in $z < -L$ involving the reflection coefficients. For the integral over $n_3 < \alpha < n_1$, we are in the situation of Fig. 3a. When we set $|R_\sigma(\alpha)|^2 = 1$, and add this to what is left of the power in $z < -L$, we find that the sum is exactly the expression of Eq. (11) (after transforming back to θ). The result is that the expression for the power is again given by Eq. (20).

For both cases (1) and (2) the power is given by the same result, Eq. (20), although the contributions come from different processes. The reason for this is that in both cases all emitted traveling waves by the multipole, corresponding to the range $0 < \alpha < n_1$, end up in the far field. In case (1) all waves are reflected and in case (2) some of the waves are transmitted, and they end up in the far field below the substrate. For these cases, no evanescent emitted waves contribute, and all emitted traveling waves contribute.

3. $0 < \varepsilon_1 < \varepsilon_3$

When $\varepsilon_3 > \varepsilon_1$ we can have the situation shown in Fig. 3c, where evanescent waves from the multipole are converted into traveling transmitted waves and end up in the far field, thereby contributing to the power. In this case we have to split the integral for the transmitted power in Eq. (13) at $\alpha = n_1$, and use the relation from Fig. 3b for the range $0 < \alpha < n_1$. For $n_1 < \alpha < n_3$, we use the relation from Fig. 3c, and the fact that in this range v_1 is pure imaginary. When compared with the expression for the power in $z > H$ we find again that the terms with $|R_\sigma(\alpha)|^2$ cancel, and that the integral of Eq. (11) shows up. The result is again Eq. (20), but now an additional term remains due to the integral over $n_1 < \alpha < n_3$ in the transmitted

power. This is the term that has its origin in the evanescent waves of the multipole.

The final result covering all cases can be written as

$$P_{1\ell m} = 1 + \frac{4\pi}{n_1} (-1)^{\ell+m} \operatorname{Re} \int_0^{n_1} d\alpha \frac{\alpha}{v_1} e^{i\beta v_1/n_1} \times [R_p(\alpha) f_{\ell m}(v_1/n_1) - R_s(\alpha) g_{\ell m}(v_1/n_1)] + \frac{4\pi}{n_1} H(\varepsilon_3 - \varepsilon_1) \operatorname{Re} \int_{n_1}^{n_3} d\alpha \frac{\alpha}{v_1} e^{i\beta v_1/n_1} \times [R_p(\alpha) f_{\ell m}(v_1/n_1) + R_s(\alpha) g_{\ell m}(v_1/n_1)], \quad (21)$$

for a magnetic multipole, and for an electric multipole we exchange the Fresnel coefficients for s- and p-waves. Here we have introduced the Heaviside step function $H(x)$ in the last term to indicate that this term only contributes for $\varepsilon_3 > \varepsilon_1$. An interesting difference between the two integrals is that the reflection coefficient for s-waves is preceded by a minus sign in the first integral but not in the second. Another difference is that the first integral has an overall factor of $(-1)^{\ell+m}$, whereas the second integral does not.

6. Dipole

For a magnetic or an electric dipole we have $\ell = 1$. Let us first consider the case $m = 0$, which corresponds to a dipole moment oriented along the z -axis. The two functions appearing in Eq. (21) are [28]

$$f_{10}(z) = 0, \quad (22)$$

$$g_{10}(z) = \frac{3}{8\pi} |1 - z^2|, \quad (23)$$

for arbitrary complex z . This yields for the emitted power by the dipole

$$P_{110} = 1 + \frac{3}{2n_1\varepsilon_1} \operatorname{Re} \int_0^{n_1} d\alpha \frac{\alpha^3}{v_1} e^{i\beta v_1/n_1} R_s(\alpha) + \frac{3}{2n_1\varepsilon_1} H(\varepsilon_3 - \varepsilon_1) \operatorname{Re} \int_{n_1}^{n_3} d\alpha \frac{\alpha^3}{v_1} e^{i\beta v_1/n_1} R_s(\alpha). \quad (24)$$

Here we notice that the integrands of both integrals are the same. When $\varepsilon_3 < \varepsilon_1$, the second inte-

gral does not contribute. Near the upper limit $\alpha = n_1$ of the first integral, the parameter v_3 is imaginary, and the corresponding transmitted wave is evanescent. For $\alpha > n_1$ also v_1 would be imaginary, corresponding to an evanescent incident wave. This gives the situation depicted in Fig. 3d, for which the Fresnel reflection coefficients are real. Then we also have that $\exp(i\beta v_1/n_1)$ is real, and due to the factor $1/v_1$ the integrand is imaginary. We can therefore extend the upper limit of integration to infinity. On the other hand, for $\varepsilon_3 > \varepsilon_1$, the second integral can be added to the first, giving an integral over the range $0 < \alpha < n_3$. Then for $\alpha > n_3$ both v_1 and v_3 are imaginary, and we are again in the situation of Fig. 3d. Therefore we can also extend the integration limit to infinity. Consequently, for all cases the result (24) can be simplified to

$$P_{110} = 1 + \frac{3}{2n_1\varepsilon_1} \operatorname{Re} \int_0^\infty d\alpha \frac{\alpha^3}{v_1} e^{i\beta v_1/n_1} R_s(\alpha). \quad (25)$$

Effectively, the upper limit of integration is $\alpha = \max(n_1, n_3)$, since for larger α the integrand is imaginary. A dipole with $m = 1$ has a dipole moment with a constant magnitude and this dipole moment rotates counterclockwise in the xy -plane. The two functions are

$$f_{11}(z) = \frac{3}{16\pi}, \quad (26)$$

$$g_{11}(z) = \frac{3}{16\pi} |z|^2. \quad (27)$$

Along similar lines we obtain

$$P_{111} = 1 + \frac{3}{4n_1\varepsilon_1} \operatorname{Re} \int_0^\infty d\alpha \frac{\alpha}{v_1} e^{i\beta v_1/n_1} \times [\varepsilon_1 R_p(\alpha) - (\varepsilon_1 - \alpha^2) R_s(\alpha)]. \quad (28)$$

The elegant representations (25) and (28) for the power emitted by a dipole have been reported numerous times in the quoted literature (for an electric dipole, so with R_s and R_p exchanged). We have derived this result by considering the field emitted by the dipole as a superposition of plane waves which reflect and refract at the interface. From this, the Poynting vector in the far field

could be found by asymptotic expansion, and after integrating over a 4π solid angle, the result for the emitted power is an expression in terms of Fresnel reflection and transmission coefficients. With the relations shown in Fig. 3, the transmission coefficients could be eliminated in favor of the reflection coefficients, and this led to the results (25) and (28) for the case of a perpendicular and a parallel dipole, respectively. It is interesting to note that these results can also be derived with a very different approach, sometimes called “radiation reaction”. In this approach one constructs an angular spectrum representation of the field emitted by the dipole and the reflected field by the interface, expressed in terms of reflection coefficients. Rather than considering the far-field solution, one considers the field at the location of the dipole. The dipole then interacts with its own field, including the reflected field, and one evaluates the emitted power by calculating the negative of the power dissipated by the dipole from its own field by integrating the corresponding term in Poynting’s theorem over a small sphere around the dipole [12]. This leads exactly to Eqs. (25) and (28). In this approach, the presence of the interface only enters through the Fresnel reflection coefficients, but the formal result is independent of the properties of the Fresnel coefficients, like the relations shown in Fig. 3. Therefore, the results (25) and (28) hold more generally, and in particular they also hold when there is absorption in the material, or when the interface structure is more complicated than the situation shown in Fig. 1. On the other hand, it is not clear how this approach can be generalized to obtain the power emitted by a multipole of arbitrary order (ℓ, m) .

7. Contribution of evanescent waves

The general result (21) splits naturally in three parts. The term “1” represents the emitted power by the multipole irrespective of the boundary and it only involves traveling waves emitted by the multipole. The first integral represents interference between the directly emitted waves and the reflected waves, and only traveling multipole waves contribute to this term. The second integral comes

from evanescent multipole waves which are converted into traveling transmitted waves by the interface. We write the power as

$$P_{\eta\ell m} = P_{\eta\ell m}^{\text{tr}} + P_{\eta\ell m}^{\text{ev}}, \quad (29)$$

indicating the contributions from traveling and evanescent multipole waves. As a measure for the relative contribution of evanescent waves we introduce the fraction

$$f = \frac{P_{\eta\ell m}^{\text{ev}}}{P_{\eta\ell m}^{\text{tr}} + P_{\eta\ell m}^{\text{ev}}} \times 100\%. \quad (30)$$

For a numerical evaluation of the emitted power, the representation given by Eq. (21) is not the most convenient, since the parameter v_1 goes to zero for $\alpha \rightarrow n_1$, leading to singularities of the integrands at $\alpha = n_1$. For the integral of the traveling part we change the integration variable according to $u = [1 - (\alpha/n_1)^2]^{1/2}$, which gives

$$P_{1\ell m}^{\text{tr}} = 1 + 4\pi(-1)^{\ell+m} \times \text{Re} \int_0^1 du e^{i\beta u} [R_p f_{\ell m}(u) - R_s g_{\ell m}(u)]. \quad (31)$$

The Fresnel coefficients have to be evaluated at $\alpha = n_1(1 - u^2)^{1/2}$. Similarly, for the evanescent part we set $u = [(\alpha/n_1)^2 - 1]^{1/2}$, which yields

$$P_{1\ell m}^{\text{ev}} = 4\pi H(\varepsilon_3 - \varepsilon_1) \times \text{Im} \int_0^{\sqrt{\varepsilon_3/\varepsilon_1 - 1}} du e^{-\beta u} [R_p f_{\ell m}(iu) + R_s g_{\ell m}(iu)], \quad (32)$$

and here the Fresnel coefficients have $\alpha = n_1(1 + u^2)^{1/2}$ as arguments.

As an example, let us consider quadrupole radiation, for which $\ell = 2$ and $m = 2, 1, 0$ (the power is independent of the sign of m). The functions f_{2m} and g_{2m} have u as their arguments in Eq. (31), but in Eq. (32) the arguments are iu , which are imaginary. For arbitrary complex z , the functions for $\ell = 2$ are given by

$$f_{22}(z) = \frac{5}{16\pi} |1 - z^2|, \quad (33)$$

$$g_{22}(z) = \frac{5}{16\pi} |1 - z^2| |z|^2, \quad (34)$$

$$f_{21}(z) = \frac{5}{16\pi} |z|^2, \quad (35)$$

$$g_{21}(z) = \frac{5}{16\pi} |2z^2 - 1|^2, \quad (36)$$

$$f_{20}(z) = 0, \quad (37)$$

$$g_{20}(z) = \frac{15}{8\pi} |1 - z^2|^2 |z|^2. \quad (38)$$

Fig. 4 shows the emitted power for an $m = 1$ electric quadrupole as a function of β , and for $\varepsilon_1 = 1$, $\varepsilon_2 = \varepsilon_3 = 4$ (single interface). Also shown are the separate contributions from traveling and evanescent waves. We see that for small distances between the surface and the multipole the emitted power is mainly due to the evanescent waves, whereas for larger distances the traveling waves determine the emitted power. Near $\beta \approx 3$ ($\beta = 4\pi$ corresponds to a distance of one optical wavelength in medium n_1), both contributions are approximately equal. Fig. 5 shows the intensity distribution for the same parameters and for $\beta = 0$. The anti-critical angle is 30° , and we notice that most radiation is emitted in the range $\theta_{ac} < \theta_t < \pi/2$, as evidenced by the large lobe. The fraction f for this distribution is 92%. Furthermore, from Fig. 4 we see that for $\beta \rightarrow 0$ the power

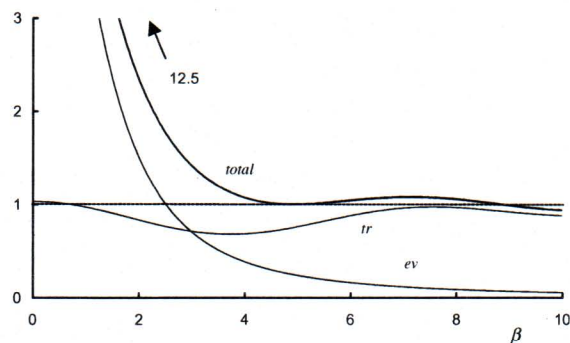


Fig. 4. The figure illustrates the dependence of the total emitted power on the normalized distance β between the multipole and the xy -plane for an $m = 1$ electric quadrupole, and for parameters $\varepsilon_1 = 1$, $\varepsilon_2 = \varepsilon_3 = 4$. Also shown are the separate contributions from traveling and evanescent multipole waves. For β small, the evanescent waves dominate the emitted power. For $\beta = 0$, the emitted power is finite, but outside the graph.

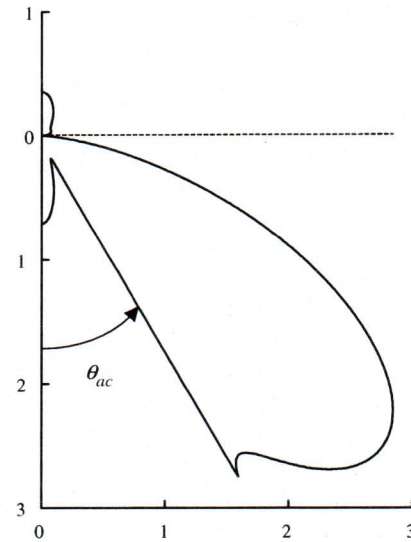


Fig. 5. Polar diagram of the intensity distribution for the same parameters as in Fig. 4. The distance between the multipole and the interface is here taken as $\beta = 0$. The anti-critical angle is 30° , and the large lobe is entirely due to evanescent multipole waves. The fraction f for these parameters is 92%.

approaches the value 12.5, which implies that the emission rate, mainly due to evanescent waves, is 12.5 times the emission rate of the same multipole in an unbounded medium.

8. Dependence on the layer thickness

The dependence of the emitted power on the layer thickness d is illustrated in Fig. 6 for an electric quadrupole and for each of the m -values. The oscillatory behavior is due to the factors $\exp(2iv_2d)$ in the Fresnel reflection coefficients. Here $v_2 = (\varepsilon_2 - \alpha^2)^{1/2}$ and α is the integration variable. For d large, the factors $\exp(2iv_2d)$ oscillate very rapidly with α , and when integrated over they average out. It was shown in Ref. [29] that the integration has the effect of averaging the reflection coefficients with the average coefficient being the Fresnel coefficient for the single ε_1 – ε_2 interface in the limit $d \rightarrow \infty$. Fig. 7 shows this effect for an electric quadrupole. However, the oscillatory behavior as a function of d is not always as prominent, as is illustrated in Fig. 8.

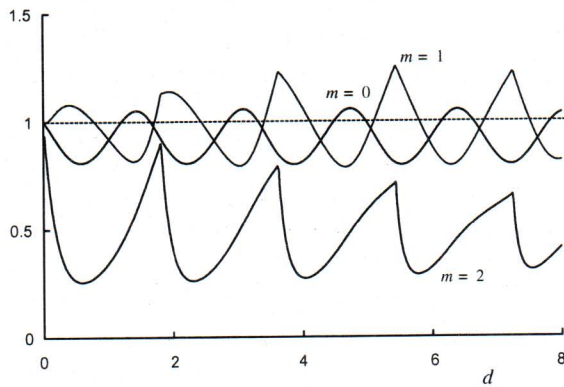


Fig. 6. Emitted power by an electric quadrupole as a function of the dimensionless layer thickness d , for $\varepsilon_1 = \varepsilon_3 = 1$, $\varepsilon_2 = 4$ and $\beta = 1$. The oscillations are due to the oscillations in the Fresnel reflection coefficients.

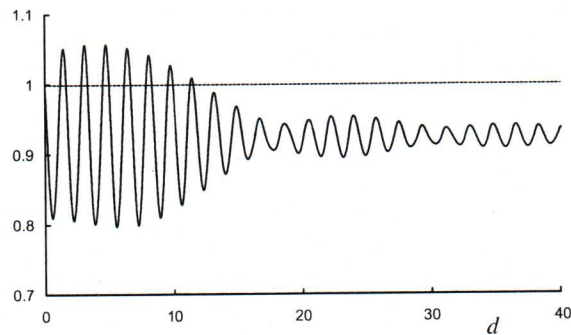


Fig. 7. Emitted power for the same parameters as in Fig. 6, but only for $m = 0$. The figure illustrates that for large d the power approaches a steady value, which is due to the fact that the fast oscillations in the Fresnel coefficients average out when integrated over.

9. Power along the xy-plane

The power emitted by the multipole, given by Eq. (21), was derived by considering the contributions from the regions $z > H$ and $z < -L$, and both contributions were combined by using the properties of the Fresnel reflection and transmission coefficients. We did not take into account the possible contributions from the radiation emitted in the regions $0 < z < H$ and $-L < z < 0$. In this section we shall show that these contributions are identically zero. The simplest argument is that the angular

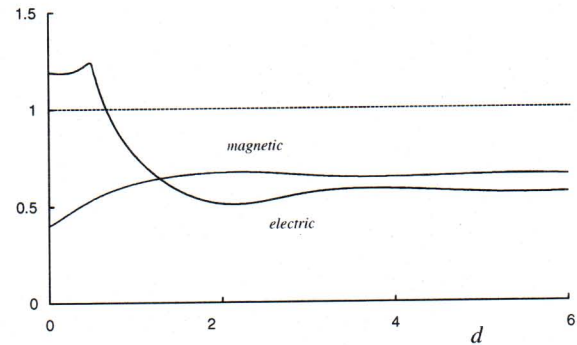


Fig. 8. This figure shows the emitted power as a function of d for an electric and a magnetic quadrupole with $m = 0$. The parameters are $\beta = \pi$, $\varepsilon_1 = 4$, $\varepsilon_2 = 1$ and $\varepsilon_3 = -2$. Near $d = 0$ there is some structure, but the curves level off rapidly with increasing d , and there are hardly any oscillations with these parameters.

width of the slab $-L < z < H$ is asymptotically zero, so the power integrated over this region vanishes asymptotically.

It is more interesting to consider the power per unit solid angle, $dP/d\Omega$, in the regions $0 < z < H$ and $-L < z < 0$. For $0 < z < H$ the electric and magnetic fields consist of *inc*-waves and *r*-waves, as schematically shown in Fig. 1. Let us consider a pair of corresponding *inc*- and *r*-waves. In the far field we have $\theta \rightarrow \pi/2$, and the wave vectors of both waves become identical and parallel to the xy -plane. For a given polarization σ , the *r*-wave has an additional Fresnel reflection coefficient $R_\sigma(\alpha_1)$ with respect to the *inc*-wave, with everything else being the same. The sum of the two waves therefore has a factor of $1 + R_\sigma(\alpha_1)$. Here, $\alpha_1 = n_1$, since $\theta = \pi/2$, and with Eq. (1) this gives $v_1 = 0$. With Eqs. (14), (15), (18) and (19) we then find

$$R_\sigma(n_1) = -1, \quad (39)$$

which gives $1 + R_\sigma(\alpha_1) = 0$. The conclusion is then that in the region $0 < z < H$ each pair of *inc*- and *r*-waves interferes destructively, and therefore the electric and magnetic fields are asymptotically zero in $0 < z < H$, and no power is emitted in this slab. The electric and magnetic fields in $-L < z < 0$ have contributions from the waves labeled “1” and “2” in Fig. 1. In the far field both waves have the same wave vector, and in this layer the parameter v_2

goes to zero for $\theta \rightarrow \pi/2$. The sum of the waves is then proportional to the sum of the two corresponding Fresnel coefficients (not given here), and it can be shown that the two waves also interfere destructively in the far zone. The proof of this is slightly more complicated since $A_\sigma \rightarrow 0$ for $v_2 \rightarrow 0$ (Eqs. (18) and (19)), and will be omitted here. Therefore, also the power emitted in the slab $-L < z < 0$ vanishes identically.

The power per unit solid angle emitted in the region $z > H$ is given by Eq. (5). When we take the limit $\theta \rightarrow \pi/2$, the Fresnel coefficients are again given by Eq. (39), and from the values of the functions $f_{\ell m}(0)$ and $g_{\ell m}(0)$ [30] we then obtain $\mathcal{N}_{\eta \ell m}(\hat{r}) = 0$ in this limit. Furthermore, for $z < -L$ the power per unit solid angle is given by Eq. (7). When we take $\theta \rightarrow \pi/2$ we have $\alpha_3 \rightarrow n_3$, so that $v_3 \rightarrow 0$. From Eq. (8) we then have $\hat{T}_\sigma(\alpha_3) \rightarrow 0$ due to the overall factor of v_3 , and therefore $\mathcal{N}_{\eta \ell m}(\hat{r}) \rightarrow 0$ for $\theta \rightarrow \pi/2$ from below the surface. In conclusion, we have $\mathcal{N}_{\eta \ell m}(\hat{r}) = 0$ in the region $-L < z < H$ and approaching this region from either above or below. The illustrations in Figs. 2 and 5 show indeed that the intensity along the xy -plane vanishes. It should be noted here that this conclusion only holds when there is an interface present. When we set $\varepsilon_1 = \varepsilon_2 = \varepsilon_3$ in, for instance, the Fresnel reflection coefficients, then $R_\sigma \equiv 0$, in conflict with Eq. (39).

10. Perfect conductor

Particularly interesting is the limit of a perfect conductor (mirror), which formally follows from $\varepsilon_2 = \varepsilon_3 \rightarrow -\infty$. Then the reflection coefficients are $R_s = -1$, $R_p = 1$.

There is no contribution from evanescent waves and the power is given by Eq. (31), which simplifies to

$$P_{\eta \ell m} = 1 + 4\pi\eta(-1)^{\ell+m} \int_0^1 du \cos(\beta u) [f_{\ell m}(u) + g_{\ell m}(u)], \quad (41)$$

where we have used that for an electric multipole the Fresnel coefficients for s- and p-polarization have to be exchanged.

When the distance between the multipole and the surface is much larger than a wavelength ($\beta \gg 1$), the factor $\cos(\beta u)$ varies very rapidly with u and integrates to zero. We then have $P_{\eta \ell m} \rightarrow 1$, as it should be. When the multipole is close to the mirror, we have $\cos(\beta u) = 1 + O(\beta^2)$, when seen as a function of β . The term “1” gives the integral of Eq. (11), and we obtain

$$P_{\eta \ell m} = 1 + \eta(-1)^{\ell+m} + O(\beta^2), \quad (42)$$

for $\beta \rightarrow 0$. The term $\eta(-1)^{\ell+m}$ equals 1 or -1 , and therefore we find for $\beta = 0$ for a magnetic multipole

$$P_{1\ell m} = \begin{cases} 0, & \ell + m \text{ odd}, \\ 2, & \ell + m \text{ even}, \end{cases} \quad (43)$$

and for an electric multipole

$$P_{-1\ell m} = \begin{cases} 2, & \ell + m \text{ odd}, \\ 0, & \ell + m \text{ even}. \end{cases} \quad (44)$$

This shows that the emission rate for a multipole on the surface of the mirror is either twice the emission rate of an unbounded multipole, or identically zero. This behavior can be understood by considering the multipole and its mirror image [24]. The mirror image of a magnetic multipole is the multipole itself for $\ell + m$ even, and for $\beta = 0$ the mirror position is the position of the multipole itself. This doubles the multipole moment, and therefore the corresponding electric field in $z > 0$ is multiplied by two, yielding a factor of four in the power as compared to the emission in $z > 0$ by an unbounded multipole. However, near the mirror all power is emitted in the direction $z > 0$, and none in the direction $z < 0$. This reduces the power by a factor of two, as compared to the unbounded multipole, giving effectively a gain of a factor of two. For $\ell + m$ odd, the mirror image of the magnetic multipole is the opposite of the multipole, and this gives effectively no multipole at all, which explains that the emission rate vanishes. For an electric multipole, the dependence on the odd- and evenness of $\ell + m$ reverses.

The functions $f_{\ell m}(u)$ and $g_{\ell m}(u)$ are given in Sections 6 and 7 for dipoles and quadrupoles, respectively. With these explicit expressions, the integral

in Eq. (41) can be evaluated for each case. We obtain for dipoles

$$P_{\eta 11} = 1 + \frac{3\eta}{2\beta} \left[\left(1 - \frac{1}{\beta^2}\right) \sin \beta + \frac{\cos \beta}{\beta} \right], \quad (45)$$

$$P_{\eta 10} = 1 - \frac{3\eta}{2\beta^2} \left(\frac{\sin \beta}{\beta} - \cos \beta \right), \quad (46)$$

and for quadrupoles

$$P_{\eta 22} = 1 + \frac{5\eta}{\beta^2} \left[\left(1 - \frac{2}{\beta^2}\right) \frac{3 \sin \beta}{\beta} - \left(1 - \frac{6}{\beta^2}\right) \cos \beta \right], \quad (47)$$

$$P_{\eta 21} = 1 - \frac{5\eta}{2\beta} \left[\left(1 - \frac{21}{\beta^2} + \frac{48}{\beta^4}\right) \sin \beta + \left(5 - \frac{48}{\beta^2}\right) \frac{\cos \beta}{\beta} \right], \quad (48)$$

$$P_{\eta 20} = 1 + \frac{15\eta}{\beta^2} \left[\left(5 - \frac{12}{\beta^2}\right) \frac{\sin \beta}{\beta} - \left(1 - \frac{12}{\beta^2}\right) \cos \beta \right]. \quad (49)$$

Fig. 9 shows the functions P_{-121} and P_{121} as a function of β . The emitted power by a multipole near a perfect conductor only depends on this parameter β . This includes the dependence on the index of refraction n_1 as a scale factor, since $\beta = 2n_1 k_0 H$.

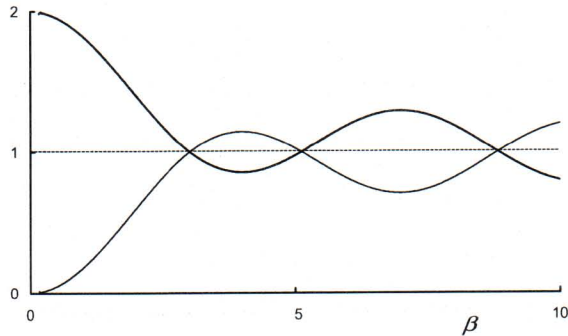


Fig. 9. Power emitted by an electric (thick line) and a magnetic (thin line) $m=1$ quadrupole near a perfect conductor as a function of the dimensionless distance β between the quadrupole and the surface. This power is given by Eq. (48). Near $\beta=0$, all negative powers of β (five orders) have to cancel, and this leads to numerical rounding inaccuracies near $\beta=0$.

11. Conclusions

Radiation emitted by an electric or a magnetic multipole consists of traveling and evanescent waves. When this multipole is located near an interface, then part of the traveling waves are emitted directly towards a detector in the far field (the *de*-waves in Fig. 1), and the remaining traveling waves of the angular spectrum serve as the incident waves on the interface (the *inc*-waves). A fraction of the *inc*-waves is reflected as traveling waves (*r*-waves), and end up in the far field in $z > H$. The remaining fraction is transmitted through the layer. For the contribution of the transmitted waves to the power we have to consider three cases, depending on the values of the dielectric constants ϵ_1 and ϵ_3 . For $\epsilon_3 < 0$, modeling a metallic substrate, the transmitted waves are evanescent and they do not contribute to the power. For $0 < \epsilon_3 < \epsilon_1$, there exists a critical angle θ_c , given by Eq. (2). Traveling *inc*-waves with an angle of incidence smaller than the critical angle give traveling transmitted waves which contribute to the power in $z < -L$, but traveling *inc*-waves with an angle of incidence larger than θ_c are transmitted as evanescent waves which die out exponentially in the substrate, and there is no contribution to the power. This corresponds to the cases shown schematically in Fig. 3b and a, respectively. For $\epsilon_3 > \epsilon_1$, there exists an anti-critical angle, given by Eq. (3), which has the significance that all incident traveling waves are transmitted in the cone $\theta_t < \theta_{ac}$, with θ_t the angle of transmission. This corresponds again to the case of Fig. 3b. In addition, there is transmission of traveling waves outside this cone, e.g., $\theta_{ac} < \theta_t < \pi/2$, and these waves have their origin in evanescent waves of the multipole field. This corresponds to the situation of Fig. 3c, and this process contributes to the power in $z < -L$.

The total power emitted by the multipole could be written in the form given by Eq. (21), which covers all possible cases. In this expression, the Fresnel transmission coefficients were eliminated in favor of the reflection coefficients by using the equations shown in Fig. 3 for the various cases. This power is normalized with the power emitted by a multipole embedded in a medium with index

of refraction n_1 , but without any boundaries. Therefore, the term “1” on the right-hand side of Eq. (21) represents the power emitted by such an unbounded multipole. It follows from the derivation of Eq. (21) that this term has contributions from *de*-waves, *r*-waves and *t*-waves. The second term in Eq. (21) is a result of interference between the *de*-waves and the specular *r*-waves. For $\epsilon_3 < \epsilon_1$, this is the only additional term, and it gives rise to an oscillatory dependence of the power on the dimensionless distance β between the multipole and the interface. For $\epsilon_3 > \epsilon_1$ there is a third term in Eq. (21), which accounts for the evanescent multipole waves that are converted into traveling waves at the interface. In the factor $\exp(i\beta v_1/n_1)$ the parameter v_1 is imaginary, and this factor has an exponential dependence on the distance β , reflecting the fact that the evanescent multipole waves decay exponentially from the multipole to the surface. Therefore, the contribution of evanescent waves decreases rapidly with increasing β , as illustrated in Fig. 4. For the intensity distribution $dP/d\Omega$ this implies that there will be no radiation outside the cone $\theta_t < \theta_{ac}$ for β sufficiently large, and this can be seen in Fig. 2. On the other hand, for β small, the emitted power originating in evanescent multipole waves, which only contribute because of the presence of the interface, can greatly exceed the power emitted by an unbounded multipole.

References

- [1] E.M. Purcell, Phys. Rev. 69 (1946) 681.
- [2] G.S. Agarwal, Phys. Rev. Lett. 32 (1974) 703.
- [3] W. Lukosz, R.E. Kunz, J. Opt. Soc. Am. 67 (1977) 1607.
- [4] W. Lukosz, R.E. Kunz, J. Opt. Soc. Am. 67 (1977) 1615.
- [5] W. Lukosz, Phys. Rev. B 22 (1980) 3033.
- [6] J.E. Sipe, Surf. Sci. 105 (1981) 489.
- [7] J.E. Sipe, J. Opt. Soc. Am. B 4 (1987) 481.
- [8] K.H. Drexhage, Prog. Opt. XII (1974) 163.
- [9] R.R. Chance, A. Prock, R. Silbey, Adv. Chem. Phys. 39 (1978) 1.
- [10] G.W. Ford, W.H. Weber, Surf. Sci. 109 (1981) 451.
- [11] P. Goy, J.M. Raimond, M. Gross, S. Haroche, Phys. Rev. Lett. 50 (1983) 1903.
- [12] G.W. Ford, W.H. Weber, Phys. Rep. 113 (1984) 195.
- [13] R.G. Hulet, E.S. Hilfer, D. Kleppner, Phys. Rev. Lett. 55 (1985) 2137.
- [14] W. Jhe, A. Anderson, E.A. Hinds, D. Meschede, L. Moi, S. Haroche, Phys. Rev. Lett. 58 (1987) 666.
- [15] D.J. Heinzen, J.J. Childs, J.E. Thomas, M.S. Feld, Phys. Rev. Lett. 58 (1987) 1320.
- [16] J. Gasper, G.C. Sherman, J.J. Stamnes, J. Opt. Soc. Am. 66 (1976) 955.
- [17] H.F. Arnoldus, J.T. Foley, Opt. Lett. 28 (2003) 1299.
- [18] H.F. Arnoldus, J.T. Foley, J. Opt. Soc. Am. A 21 (2004) 1109.
- [19] J.D. Jackson, Classical Electrodynamics, third ed., Wiley, New York, 1999, p. 429.
- [20] M.E. Rose, Multipole Fields, Wiley, New York, 1955.
- [21] J.M. Eisenberg, W. Greiner, Excitation Mechanisms of the Nucleus, North-Holland, Amsterdam, The Netherlands, 1970 (Chapter 3).
- [22] M.E. Rose, Elementary Theory of Angular Momentum, Dover, New York, 1995 (Chapter 7).
- [23] A.J. Devaney, E. Wolf, J. Math. Phys. 15 (1974) 234.
- [24] H.F. Arnoldus, J. Math. Phys., submitted for publication.
- [25] A. Erdélyi, Physica 4 (1937) 107.
- [26] G.C. Sherman, J.J. Stamnes, É. Lalor, J. Math. Phys. 17 (1976) 760.
- [27] M. Born, E. Wolf, Principles of Optics, seventh (expanded) ed., Cambridge University Press, Cambridge, England, 1999, Appendix III, p. 890.
- [28] H.F. Arnoldus, J. Opt. Soc. Am. A, in press.
- [29] H.F. Arnoldus, Surf. Sci. 444 (2000) 221.
- [30] H.F. Arnoldus, J.T. Foley, Opt. Commun., submitted for publication.